

A positron source using an axially oriented crystal associated to a granular amorphous converter

XU Cheng-Hai(徐成海)^{1,2} Robert Chehab³ Peter Sievers⁴ Xavier Artru³
Michel Chevallier³ Olivier Dadoun² PEI Guo-Xi(裴国玺)¹
Vladimir M. Strakhovenko⁵ Alessandro Variola²

¹ Institute of High Energy Physics, Chinese Academy of Sciences, Beijing 100049, China

² Laboratoire de l'Accélérateur Linéaire, IN2P3/CNRS et Université de Paris-Sud, BP 34-91898, Orsay cedex, France

³ Institut de Physique Nucléaire de Lyon, IN2P3/CNRS et Université Lyon 1, 69622 Villeurbanne, France

⁴ CERN, CH-1211, Genève 23, Switzerland

⁵ Budker Institute of Nuclear Physics, Av. Lavrentyeva, 11, 630090 Novosibirsk, Russia

Abstract: A non-conventional positron source using the intense γ radiation from an axially oriented monocrystal which materializes into e^+e^- pairs in a granular amorphous converter is described. The enhancement of photon radiation by multi-GeV electrons crossing a tungsten crystal along its $\langle 111 \rangle$ axis is reported. The resulting enhancement of pair production in an amorphous converter placed 2 meters downstream, is also reported. Sweeping off the charged particles from the crystal by a bending magnet upstream of the converter allows a significant reduction of the deposited energy density. Substituting a granular target made of small spheres for the usual compact one, makes the energy dissipation easier. The deposited energy and corresponding heating are analyzed and solutions for cooling are proposed. The configurations studied here for this kind of positron source allow its consideration for unpolarized positrons for the ILC.

Key words: channeling effect, crystal, positron source, ILC

PACS: 41.74.Ht, 07.77.Ka **DOI:** 10.1088/1674-1137/36/9/014

1 Introduction

The use of axially oriented crystals with GeV electron beams in channeling conditions provides powerful sources of (unpolarized) photons. These photons can then materialize into e^-e^+ pairs in the same crystal or in amorphous converters put downstream. Theoretical studies [1] and simulations [2–4] were confirmed by experiments at CERN and KEK [5–9]. Separating the crystal-radiator from the amorphous-converter with a bending magnet in between to sweep off the charged particles, allowing only photons to impinge on the converter, presents very interesting features concerning the amount of energy deposited and for its density [10]. For such a device, called a hybrid source, the amount of PEDD (Peak Energy Deposition Density) can be made lower than critical values (35 J/g, for W) avoiding the use of a multi-target system; that was already proposed and adopted for CLIC for its baseline [11]. However, the problem of

very intense beams as for ILC may present a serious problem for the target survival. We have carried out a study on a particular kind of converter made of granular substance (W spheres) which presents the advantages of easier thermal dissipation; it was already considered for targets submitted to high intensity proton beams and dedicated to neutrino factories (P. Sievers, [12]). Some results concerning a hybrid target with a granular converter are presented here.

2 The hybrid source

A high energy electron beam (5 to 10 GeV) is directed along the crystal axis. Photons, electrons and positrons are generated. A sweeping magnet takes off the charged particles and only the photons impinge on the amorphous converter (Fig. 1). The distance may be about 2 meters. For the ILC, we consider an electron beam of 10 GeV with a transverse r.m.s

Received 6 December 2011, Revised 16 January 2012

©2012 Chinese Physical Society and the Institute of High Energy Physics of the Chinese Academy of Sciences and the Institute of Modern Physics of the Chinese Academy of Sciences and IOP Publishing Ltd

radius of 2.5 mm. A scheme of the hybrid source is presented on Fig. 1.

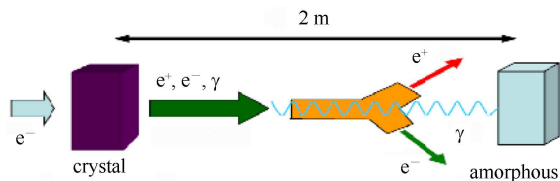


Fig. 1. The hybrid positron source.

2.1 The crystal radiator

The idea of substituting an oriented crystal for the magnetic undulator in order to produce an intense source of photons was generated more than twenty years ago [13]. Two main arguments prevailed: the very strong fields available on the atomic rows of the crystal, equivalent to 10^3 Tesla and the short periods associated with the oscillating trajectories of the electrons along the crystal axes (~ 1 μm). The latter characteristics allows tens of MeV photon energy to be reached with a GeV electron beam incident on the crystal; that represents two orders of magnitude less energy than for an undulator having cm period.

The energy spectrum and the yield of the photons produced in the crystal depend, obviously, on the electron incident energy. For that, it is interesting to consider a figure of merit [1] given by the ratio:

$$R = I_{\text{ch}}/I_{\text{br}}, \quad (1)$$

where I_{ch} is the intensity of channeling radiation and I_{br} , that of bremsstrahlung. This ratio depends on the electron energy and on the crystal. For instance, $R=1$ for the axis $\langle 111 \rangle$ at 0.7 GeV for W, 1.3 GeV for Si and 1.9 GeV for Ge. At much higher energies, $R \gg 1$ and the crystal effects dominate on bremsstrahlung and R is growing very fast with the energy. The radiation yield depends also on the crystal thickness. Increasing the crystal thickness, one may meet saturation due to the multiple scattering and the decrease in energy of the radiating particles.

Another peculiarity of the channeling radiation is that the emitted photons are much softer in energy than those created by bremsstrahlung. Therefore, the channeling radiation may be more efficient than bremsstrahlung, even with $R=1$, providing a larger number of photons. For the application foreseen here, the ILC positron source, we have chosen an incident energy of 10 GeV and a W crystal, with $\langle 111 \rangle$ axial orientation and 1 mm thickness. To fulfill good channeling operation, the following conditions are required:

- 1) A mosaic spread lower than the channeling critical angle
- 2) An incident beam divergence, lower than the channeling critical angle.

This critical angle is given by:

$$\Psi_c = [2U_o/E]^{1/2}, \quad (2)$$

where U_o is the depth of the potential well created by the atomic rows and E the electron energy. For our conditions (10 GeV, $\langle 111 \rangle$ W axis) the critical angle is ~ 0.5 mrad.

2.2 The granular converter

The very intense incident electron beam considered in the linear collider projects (10^{14} e^- /second) requires resistant targets. In the muon collider and neutrino factories projects, a similar situation is met with powerful proton beams impinging on targets to produce pions decaying into muons and then into neutrinos. P. Sievers and P. Pugnat have proposed the use of granular targets made of a great quantity of small spheres [12]. The high ratio of surface/volume of the spheres ($\sim 3/r$) makes the thermal dissipation easier. In the scheme considered for the converter of the hybrid source, the spheres are arranged in staggered rows. An example is shown in Fig. 2.

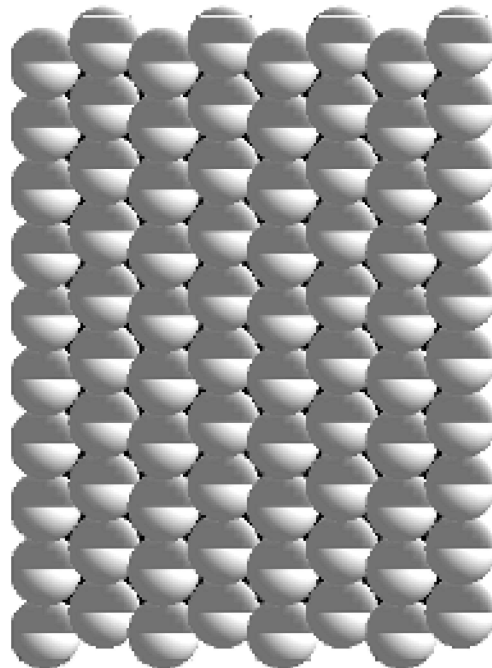


Fig. 2. A granular target: 8 rows of $r=1$ mm spheres.

The choice of the number of rows is related to two essential quantities:

- 1) The required positron yield
- 2) The Peak Energy Deposition Density (PEDD)

Table 1. Comparison of compact and granular targets.

	thickness/mm	yield (e^+/e^-)	PEDD/ ($\text{GeV}/\text{cm}^3/e^-$)	ΔE dep./ (MeV/e^-)	N -layer	sphere number	effective density/ (g/cm^3)
compact	8	13.3	2.24	523			19.3
granular $r=1$ mm	10.16	12.5	1.81	446	3	864	13.9
granular $r=0.5$ mm	11.60	13.45	2.33	613	7	8064	13.9

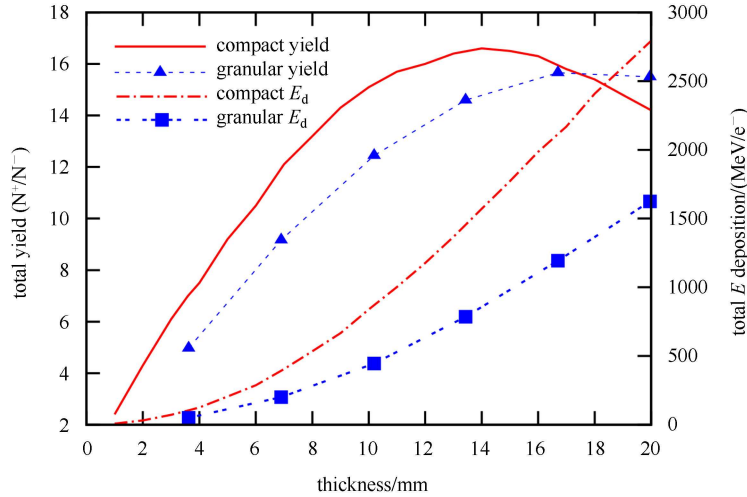


Fig. 3. Comparison of compact and granular targets.

For that purpose, we have made a comparison of two choices of granular targets ($r=1$ mm and $r=0.5$ mm) with a compact target 8 mm thick which was convenient for the required positron yield. This comparison is shown in Table 1.

We can observe that the “3 layers” granular target has almost 6% less positron yield than the compact target but 20% lower PEDD. It looks more interesting from that point of view than the $r=0.5$ mm granular solution. These considerations may also be derived from Fig. 3, where the total yield and energy deposited normalized to the incident electron are reported in the function of the target thickness expressed in mm or in number of layers.

We can see that the deposited energy for the “3 layers” target is 446 MeV/ e^- whereas it is 523 MeV/ e^- for the 8 mm compact target.

3 The simulations

The simulations have been operated with two programmes:

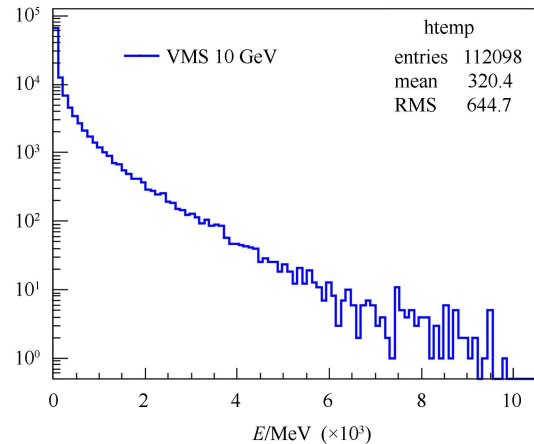
1) A programme (VMS) describing the crystal effects (channeling, coherent bremsstrahlung, pair creation...) written by V. M. Strakhovenko [14].

2) The GEANT4 code which uses the outputs of the first programme as event generator; results on positron production are provided by GEANT4.

Crystal effects are also described by the programme FOT; the results agree with VMS.

3.1 The results on photons from the crystal

The photon characteristics are obviously important for the positron generation. We represent in Fig. 4 the energy spectrum in the case of a 10 GeV

Fig. 4. The photon energy spectrum ($E^- = 10$ GeV; $L=1$ mm W crystal).

incident electron beam on a 1 mm thick crystal target oriented on its $\langle 111 \rangle$ axis. In Fig. 5, we have represented the transverse characteristics of the photon beam impinging on the granular converter. These photons have been created by an electron beam having an r.m.s radius of 2.5 mm and an energy of 10 GeV. The r.m.s photon beam radius at the target is ~ 3.5 mm.

3.2 Simulation results on positrons

3.2.1 The positron beam

The positrons created in the granular target (3 layers) are captured by an adiabatic matching device (AMD) which exhibits a slowly decreasing axial magnetic field from the converter to the entrance of the first accelerating section. The field is tapering from

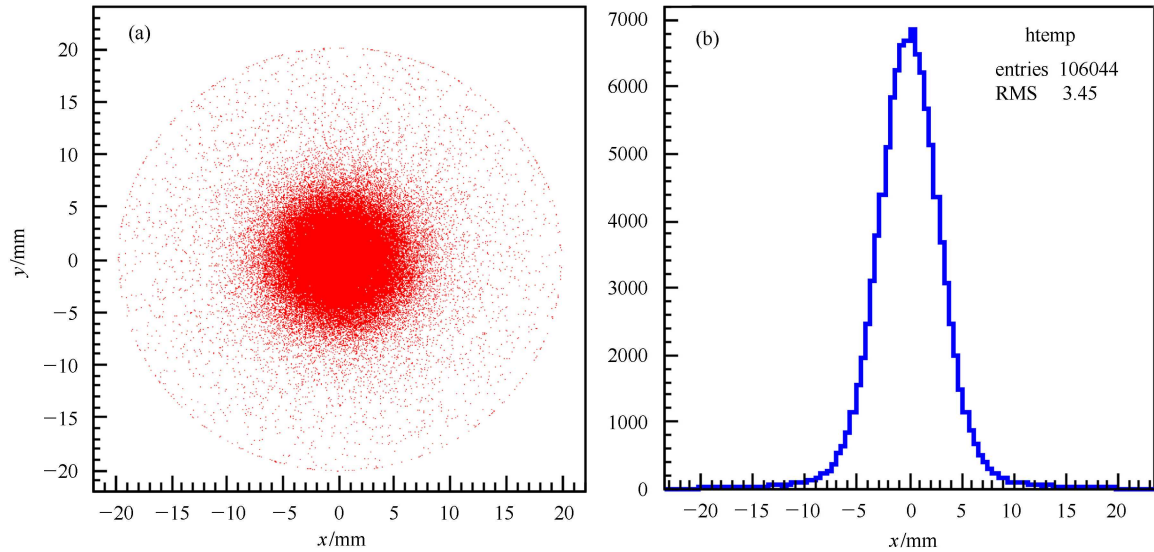


Fig. 5. The transverse characteristics of the photon beam at the converter; (a) x - y distribution; (b) Marginal y distribution on x plane; beam dimensions are given in mm.

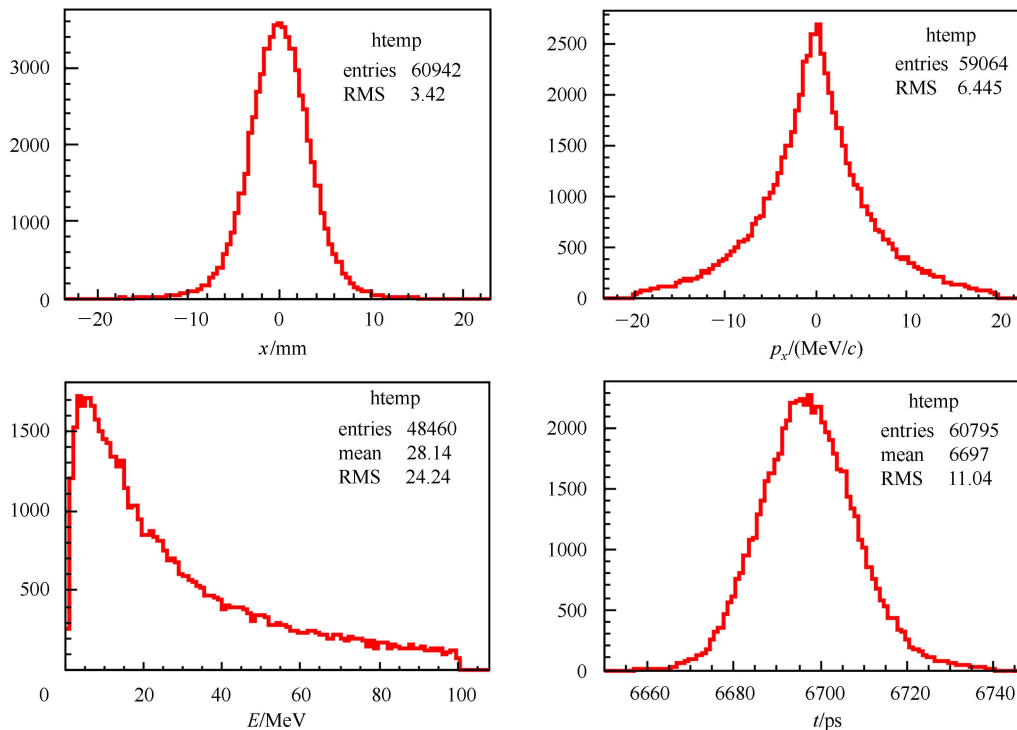


Fig. 6. The transverse dimensions and momentum, energy spectrum and time distribution at the target exit.

6 tesla to 0.5 tesla over 50 cm. We present in Fig. 6 the energy spectrum, transverse dimension and momentum and time distribution at the converter exit. The same kind of figure (Fig. 7) concerns the same parameters after the capture by the AMD and one meter acceleration. We can observe the phase space transformation due to the matching device converting the small dimensions and large transverse momentum at the converter into larger dimensions and smaller transverse momentum after the AMD and one meter acceleration.

3.2.2 Energy deposited and PEDD

The configuration chosen for the linear collider ILC is based on a pulse time structure modification before the target in order to decrease the power deposited per pulse; the nominal structure of the ILC beam is then recuperated after the damping ring. For that purpose, we have chosen the configuration proposed by T. Omori from KEK [15] and where the incident electron beam is made of minitrains of 100 bunches each with a periodicity of 300 Hz in a macropulse of 40 ms containing 13 minitrains. See Fig. 8.

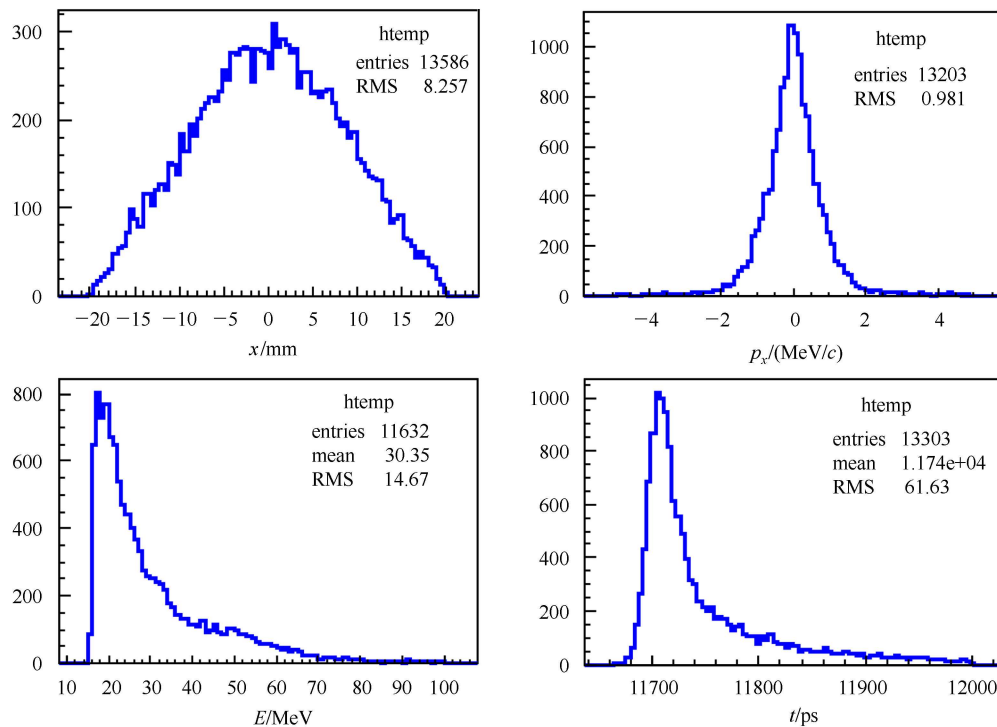


Fig. 7. The transverse dimensions and momentum, energy spectrum and time distribution after acceleration.

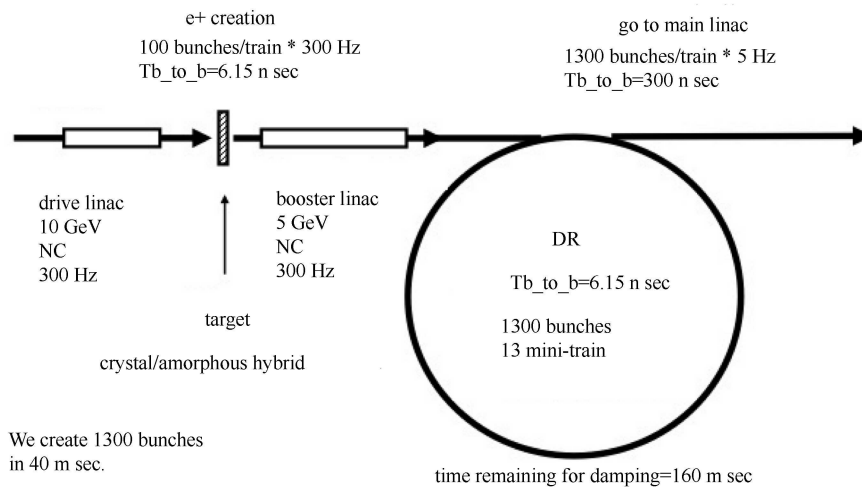


Fig. 8. The scheme of the 300 Hz solution proposed by Omori et al.

The first target submitted to the incident beam is the crystal. An estimation of the energy deposited and of the PEDD is necessary.

The 10 GeV electron beam with an r.m.s beam radius of 2.5 mm deposit about 8 MeV/e⁻ in the 1 mm thick W crystal. That represents a power of 160 watts. Cooling is foreseen. The energy deposition density has a peak (PEDD) of 0.35 GeV/cm³/e⁻. That represents for the ILC beam a PEDD of 5.8 J/g for a minitrain of 2×10¹² impinging e⁻. The minitrains are separated by 3.3 ms, giving enough time for the relaxation of shock waves.

Another problem for the crystal concerns the high rate of Coulomb scattering on the nuclei which could lead to dislodgements and affect the crystal structure. The fluence is 2×10¹⁶ e⁻/mm²/hour. It needs about 100 hours to reach the fluence obtained in the SLAC test in 1997 where no damage was observed on the crystal [16]. Estimating the critical fluence one order of magnitude larger, leads to a working time of a thousand hours without estimated damage. Annealing procedures help to restore the crystal qualities.

The crystal must be cooled. It can be mounted in a water cooled round frame (a) (radially constrained) or mounted on only one side (with vertical but no horizontal expansion). The target unit (crystal + Be-windows) could also be cooled by a He jet (b), the heat being evacuated through both side faces of the crystal. This allows devising a support for the crystal which provides the required stability in its orientation, but permits its unconstrained lateral thermal expansion, to reduce thermal stresses and fatigue. Five crystals can be put on a transversely moving frame: that will reduce the average power deposited whereas the PEDD per micropulse (0.6 μs) and per macropulse (40 ms) will not change. The fluence associated with radiation damage is decreased by a factor of 5. This choice is compatible with the use of a goniometer in which a horizontal motion is foreseen with the two rotations (H and V axes). The device is shown in Fig. 9. The translation direction is perpendicular to the plane of the figure.

The amorphous converter is the target where the energy deposition is very important due to the large number of secondaries. For the chosen system (300 Hz) we have determined the energy deposition density in the (*x*, *z*) plane; where *z* is the propagation axis. The spheres have 1 mm radius and correspond to a volume of 4 mm³. The largest value (PEDD) is 1.8 GeV/cm³/e⁻; it is slightly lower than that of a compact target. The PEDD corresponding to a minitrain is about 30 J/g. The total energy deposited in

the target is ~446 MeV/e⁻ for the 3 layers target. The deposited energy density is presented in Fig. 10. The vertical scale is in GeV/cm³/e⁻.

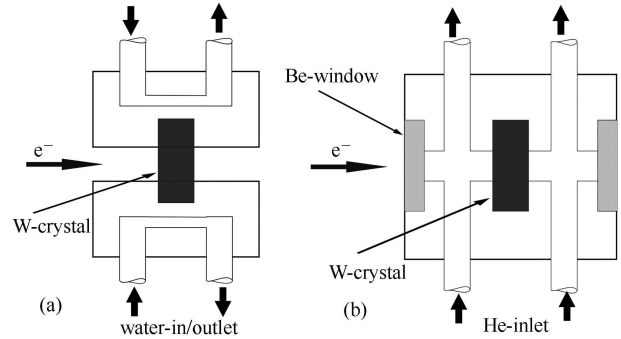


Fig. 9. The crystal mounting with the two cooling options: water cooling and He jet cooling.

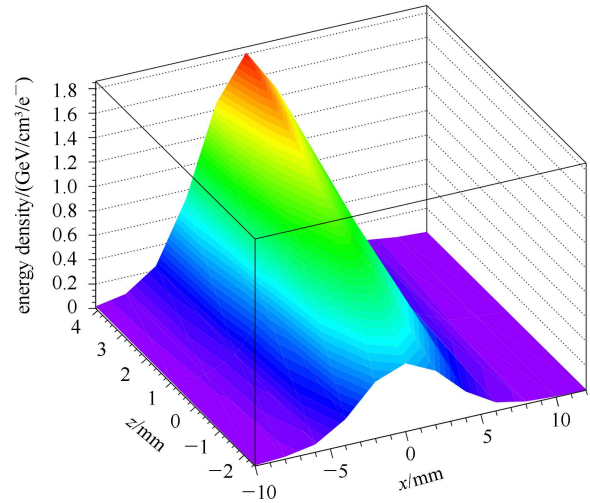


Fig. 10. Energy deposition density in the 3 layers granular converter. Beam direction is indicated (*z* axis). Maximum density is at the target exit.

4 Heating and cooling for the granular converter

In granular targets, consisting of densely packed spheres with sizes smaller than the r.m.s transverse beam profile of 3.5 mm, only small and essentially constant temperature gradients will be created across each individual sphere. Therefore, the spheres will be able to expand relatively freely and will be submitted to negligible thermal stresses.

Thermally induced shocks can be neglected when: $r/2 \ll t_o c$; *r*: radius of the sphere of 1 mm; *t_o*: pulse duration of a micro pulse of 0.6 micro seconds; *c*: velocity of sound in tungsten: $c = 4 \times 10^3$ m/s. For ILC this is satisfied in good approximation.

Another important feature of the granular target is that the deposited heat can be evacuated rapidly and at the location of heat deposition by the cooling fluid passing between the spheres. Excluding a stationary target, two solutions have been considered:

- 1) The rotating wheel
- 2) The pendulum

An overview of the thermal problems associated with this kind of e^+ source is found in Ref. [17].

4.1 A granular target on a rotating wheel

A stationary target would receive too large an amount of deposited energy, leading to serious heating problems. To reduce the adiabatic temperature rises induced by one macro pulse, the beam energy can be diluted by sweeping, rotating the target. Since the deposited beam energy is concentrated within a diameter of about 1 cm (see previous plot), with a linear velocity of the rim of the rotating wheel of about 3 m/s, the rim is displaced by 1 cm over 3.3 ms, so the energy of each minitrain is separated from the adjacent, following minitrain. Only very little pile up occurs. The calculated maximum temperature rise in the target rim, resulting from the PEDD per minitrain, is not exceeding 222 K. Details on the wheel and on the target container (Be and Ti) are presented below.

Beryllium 1 mm thick is chosen for the entrance and exit windows; Titanium 1 mm thick is chosen for the upper and lower parts of the container. Energy deposited and PEDD have been evaluated for the windows; they are negligible for Ti, whereas for Be the PEDD represents 30.6 J/g (downstream window) leading to sustainable temperature rise of about 15 K/minitrain. The rotating wheel is represented in Fig. 11. To minimize the temperature rise in helium during its passage along the periphery, its path length should be minimized by increasing the number of spokes for the He inlets and outlets.

The minimum periphery of the rotating wheel would be 13 cm, i.e. a diameter of 4 cm, to distribute uniformly a macro pulse over its rim over 40 ms. This results in a rotation frequency of 23 Hz or 1400 r.p.m, which may be difficult to achieve with rotating seals for the He inlets and outlets.

Therefore a larger wheel with a diameter of 58 cm is considered. With a velocity of the rim of 3.25 m/s, allowing for comfortable separation between minitrains, this leads to a rotation at 1.786 Hz or 107 r.p.m. which will be much easier to engineer. 3×10^6 pulses will be accumulated per target over 100 days of operation. With this configuration and taking into

account the repetition frequency of the macro pulses of 5 Hz, it results that, on average, each sphere will be hit every 5 turns, i.e. every 2.8 s. The total, average power, to be removed from a wheel (as from a stationary target) is about 10 kW. With helium, pressurized to 1 MPa and with an entrance velocity of 10 m/s, a He mass flow of 30 gr/s is required which would result in an average temperature rise of 84 °C at the exit of the He-flow. Temporarily and locally, values of 250 °C in the He may, however, occur at the hottest sphere just after a minitrain. Clearly, the wheel must be made vacuum tight and resist the internal He-pressure of 1 MPa. Moreover, with the above specified He-cooling, the time constant of the exponential decrease in temperature of an adiabatically heated sphere is about 100 ms. Thus, a sphere will be cooled to practically zero before being hit again after 2.8 s.

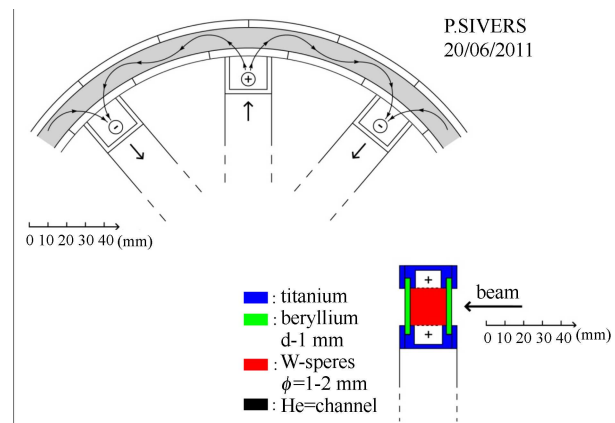


Fig. 11. The rotating wheel.

4.2 Eddy currents

Interference of the magnetic fringe field of the flux concentrator with the adjacent rotating wheel has been studied for fast rotating wheels (I. Bailey). With the above velocity ~ 3 m/s, this problem should be much reduced. Anyway, this must be confirmed by further studies.

4.3 The pendulum

To avoid rotating seals, wobbling or trolling targets have been devised at Durham ILC e^+ Meeting in October 2009, where the displacement of the target structure from the outside into the vacuum is made via flexible, vacuum tight bellows. The injection of the cooling fluid can thus be ensured through a rigid, non-rotating structure. In the following we consider a “Pendulum Target”, where the required displacement

and velocity are provided by the sinusoidal oscillation of the target (Fig. 12). The width of the target is 13 cm, providing a space for 13 minitrains with a diameter of 1 cm each and being displaced, when the beam is hitting the target, at a velocity of about 3 m/s over ± 7.5 degrees. The total swing is ± 23 degrees, allowing comfortable inversion of the direction of the movement during the “off beam” time of 160 ms. The same range in angle must be sustained by the bellows oscillating at 2.5 Hz. Since in this configuration the average time between hits of the same target spot is about 0.2 s as compared with the rotating wheel with 2.8 s, an average temperature higher by about 100 K will result. This might, if necessary, be compensated by an improved He cooling. Clearly, prototyping will be required, also to assess the life time of the spheres, the windows and the bellows, submitted to 4×10^7 . The cycle of continuous operation is over 100 days.

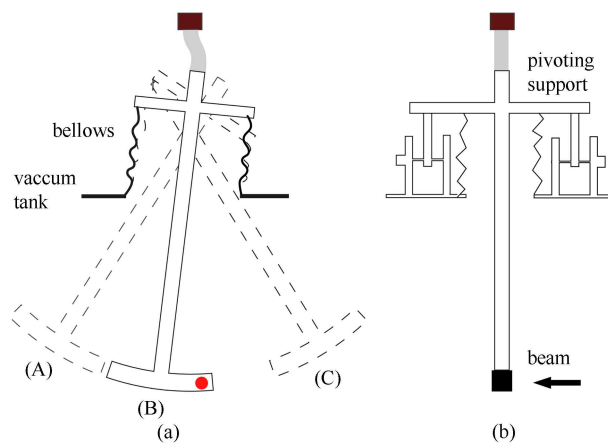


Fig. 12. The pendulum for a granular target.

5 Summary and conclusions

The hybrid target with a granular amorphous converter exhibits:

- 1) A good quality positron beam (yield, emittance) generated by photons from channeling radiation
- 2) The PEDD for the granular converter is lower than for the compact one
- 3) An efficient thermal dissipation process due to the granular character.

In particular, the enlargement of the macro pulse to 40 ms duration in the above-considered “300 Hz KEK-System” and leaving a gap of “no-beam” of 160 ms, sufficient for efficient damping, opens the possibility to reduce the thermal load from the macro pulse on the target by displacing it laterally through rotation or trolling it. Lateral velocities of about 3 m/s for this displacement are sufficient to reduce the local energy deposition density by a factor of 13 (in one macropulse). Using granular targets, consisting of an ensemble of Tungsten spheres of 2 mm in diameter or below and cooled by a helium gas stream passing between the spheres, tolerable temperatures for tungsten, helium and the target container are achieved. In addition to a rotating wheel, a pendulum target is considered, by which the use of rotating vacuum and He-seals is avoided. Both target types seem to represent viable solutions for the positron production in the considered ILC scheme.

The authors are indebted to T. Suwada, T. Kamitani, T. Omori, J. Urakawa (KEK), T. Takahashi (Hiroshima University), L. Rinolfi, A. Vivoli (CERN) for valuable discussions.

References

- 1 Baier V N, Katkov V M, Strakhovenko V M. Phys. Stat. Sol. (b), 1986, **133**: 583–592
- 2 Artru X, Baier V N, Chehab R et al. Nucl. Instrum. Methods A, 1994, **344**: 443–454
- 3 Artru X et al. Nucl. Instrum. Methods B, 1996, **119**: 246–252
- 4 Artru X, Chehab R, Chevallier M et al. Phys. Rev. ST Accel. Beams, 2003, **6**: 091003
- 5 Chehab R et al. Phys. Lett. B, 2002, **525**: 41–48
- 6 Artru X et al. Nucl. Instrum. Methods B, 2003, **201**: 243–252
- 7 Artru X et al. Nucl. Instrum. Methods B, 2005, **240**: 762–776
- 8 Suwada T et al. Phys. Rev. E, 2003, **67**: 016502
- 9 Suwada T et al. Phys. Rev. ST Accel. Beams, 2007, **10**: 073501
- 10 Artru X, Chehab R, Chevallier M et al. Nucl. Instrum. Methods B, 2008, **266**: 3868–3875
- 11 Artru X et al. Il Nuovo Cimento C, 2011, **34**(4): 141–148
- 12 Sievers P, Pugnati P. J. Phys. G: Nucl. Part. Phys., 2003, **29**: 1797–1800
- 13 Chehab R et al. Proceeding of PAC89. Chicago 1989. 283–285
- 14 Baier V N, Katkov V M, Strakhovenko V M. Nucl. Instrum. Methods B, 1995, **103**: 147–155
- 15 Omori T. The 300 Hz Generation Option of ILC Positron Source. Proceedings of POSIPOL 2009 Workshop. Lyon, 2009
- 16 Chehab R et al. Radiation Damage Study of a Monocrystalline Tungsten Converter. Proceedings of EPAC’98. Stockholm, 1998
- 17 Sievers P et al. Positron Source Using Channeling with a granular Converter. Proceedings of POSIPOL 2011 Workshop. Beijing, 2011